# Elucidation, by Scanning Microcalorimetry, of the Detailed Mechanism of the Thermal Rearrangement of [18]Annulene into Benzene and 1,2-Benzo-1,3,7-cyclooctatriene. Determination and Interpretation of the Thermochemical and Kinetic Parameters of the Three Consecutive Reactions Implicated

**Jean F. M. Oth*,†**

*Laboratory for Organic Chemistry, Swiss Federal Institute of Technology, CH-8006 Zürich, Switzerland*

**Jean-Marie Gilles‡**

*Physics Department, Facultés Universitaires N.-D. de la Paix, B-5000 Namur, Belgium*

*Received: February 3, 2000*

The thermograms $\dot{Q}_r(T)$ recorded for the thermal rearrangement of [18]annulene **1** have been reinvestigated using an iterative method (CALIT-3 program) based on the numerical integration of the kinetic equations established for the following reaction mechanism: [18]annulene **1** $\xrightarrow{k_1}$ tetracyclic intermediates **2** $\xrightarrow{k_2}$ *trans*-bicyclo[6.4.0]dodeca-2,4,6,9,11-pentaene **3** + benzene **5**; **3** $\xrightarrow{k_3}$ 1,2-benzo-1,3, 7-cyclooctatriene **4**. Independent $^{13}$C-NMR experiments indicate that three chiral tetracyclic intermediates **2a**, **2b**, and **2c** are implicated in the reaction. They are considered to play the same role in the mechanism and are therefore considered as a single compound **2** in the kinetic equations. A programmed differential microcalorimeter with linearly increasing temperature was used for producing the thermograms. The reaction enthalpies $\Delta_{r,i}H$ of each individual reaction ($i$ = 1, 2, or 3) as well as the Arrhenius parameters $E_{a,i}$, log $A_i$ and the activation thermodynamic quantities $\Delta H^{\ddagger}_i$, $\Delta S^{\ddagger}_i$, and $\Delta G^{\ddagger}_i$ (at 298.2 K) have been established by the iterative numerical simulation of the thermograms. These results are discussed. The enthalpy of formation of [18]annulene **1**, as well as the stabilization and $\pi$-bond delocalization energies of this molecule have been deduced: $\Delta H^{\circ}_f$(**1**, g, 298.2 K) = 123.4 ± 3.7 kcal mol$^{-1}$; $\Delta H_{stab}$(**1**) = − 37.6 ± 4.5 kcal mol$^{-1}$; $\Delta H_{deloc}$($\pi$-bonds in **1**) ≃ − 120.5 kcal mol$^{-1}$. The stabilization enthalpy $\Delta H_{stab}$(**1**) has been used for discussing the activation enthalpy of the conformational mobility in **1** previously reported. The pathway multiplicities deduced from the detailed mechanisms for each individual reaction are discussed in view of the interpretation of the large activation entropies found. Of special interest is the discussion of the mechanism of the two suprafacial 1,5 hydrogen shifts implied in the reaction **3** $\xrightarrow{k_3}$ **4** and of the high activation entropy observed. In independent measurements, the rate of disappearence of the [18]annulene **1** has been followed by UV spectroscopy in order to obtain the kinetic parameters for the first reaction. The results of these independent measurements are in good agreement with those obtained by the analysis of the thermograms. The reported investigation points to the fact that the thermograms recorded with our calorimetric method constitute very precise data and that their correct analysis allows the elucidation of complex reaction mechanisms.

## I. Introduction

The thermal rearrangement of [18]annulene **1** has been investigated by one of us by scanning calorimetry,[1] and the final products have been identified as benzene **5** and 1,2-benzo-1,3,7-cyclooctatriene **4**. The analysis of the thermograms recorded allowed the determination of the enthalpy of formation and the stabilization energy of [18]annulene **1**, but the details of the rearrangement mechanism were not elucidated.

The thermograms were analyzed as being the result of a one-step first-order reaction (program CALIT-2 [2]) since their habitus is in accordance with this interpretation, although we have recognized the implication of tetracyclic intermediate(s) in the reaction mechanism. The development of an iterative computation program to simulate thermograms observed for successive first-order reactions or for successive and parallel first-order reactions (program CALIT-3 [3]) led us to reinvestigate the thermograms.

We report here on the mechanism of the thermal rearrangement of [18lannulene elucidated via the simulation of the thermograms, the iterative computations being conducted with the CALIT-3 program considering three successive first-order reactions. Further kinetic measurements were undertaken that substantiate the results of this ultimate analysis of the thermograms. These results lead us to the following conclusion:

A thermogram measured with our calorimeter gives the value of the reactions heat flux $\dot{Q}_r$ as a function of the sample temperature, which is increased linearly with time. It consists of a great number of data points and contains very precise kinetic information. Even when its shape does not exhibit direct

† Tannenweg 8, CH-8908 Hedingen, Switzerland.
‡ Rue de Namur 13, B-1435 Mont-St-Guibert, Belgium.

10.1021/jp000443p CCC: $19.00 
Published on Web 08/09/2000

evidence of the complexity of the reaction mechanism, the thermogram, when properly analyzed, allows the elucidation of the mechanism of the rearrangement investigated and the determination of the thermochemical and kinetic parameters characterizing each individual reaction implicated.

## II. The Thermal Rearrangement of [18]Annulene

In our calorimetric technique,[4] the compound to be investigated is in solution in a deuterated solvent, the solution being introduced in an ampoule made of 8 mm o.d. precision NMR tube and sealed under vacuum (45 mm length). The purity of the compound is checked by NMR before the thermolysis, the ampule being introduced in a 10 mm NMR tube and the temperature of the NMR probe being adequately selected. The nature of the reaction product(s) is determined in the same manner after completion of the calorimetric measurement. Figure 1 reproduces the spectra recorded before and after run 105 in the calorimeter.

The spectrum recorded at −30 °C before the run in the calorimeter confirms the high purity of the [18]annulene **1**; the spectrum measured after pyrolysis indicates the formation of benzene **5** and of 1,2-benzo-1,3,7-cyclooctatriene **4**. The spectrum of 1,2-benzo-1,3,7-cyclooctatriene was known to us from our studies on [12]annulene:[5] upon photolysis at $\lambda = 350$ nm and −70 °C, [12]annulene gives *trans*-bicyclo[6.4.0]dodeca-2,4.6,9,11-pentaene **3**, which rearranges thermally in 1,2-benzo-1,3,7-cyclooctatriene **4**.[6] In a first step we have analyzed the thermograms according to the reaction represented in Scheme 1.[3]

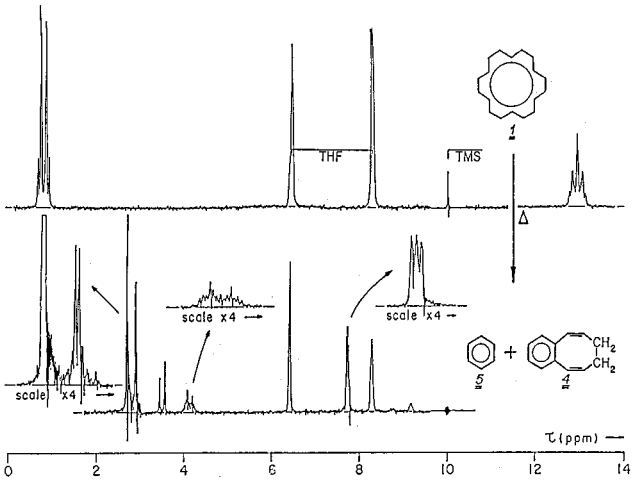


**Figure 1.** $^1$H-NMR spectra of a solution of [18]annulene in tetrahydrofuran-$d_8$ before (spectrum at −30 °C) and after (spectrum at +30 °C) run 105 in the calorimeter (100 MHz, TMS as reference signal).

Figure 2 reproduces thermogram 105 recorded with 0.423 deg/min heating rate. The thermogram was simulated, after

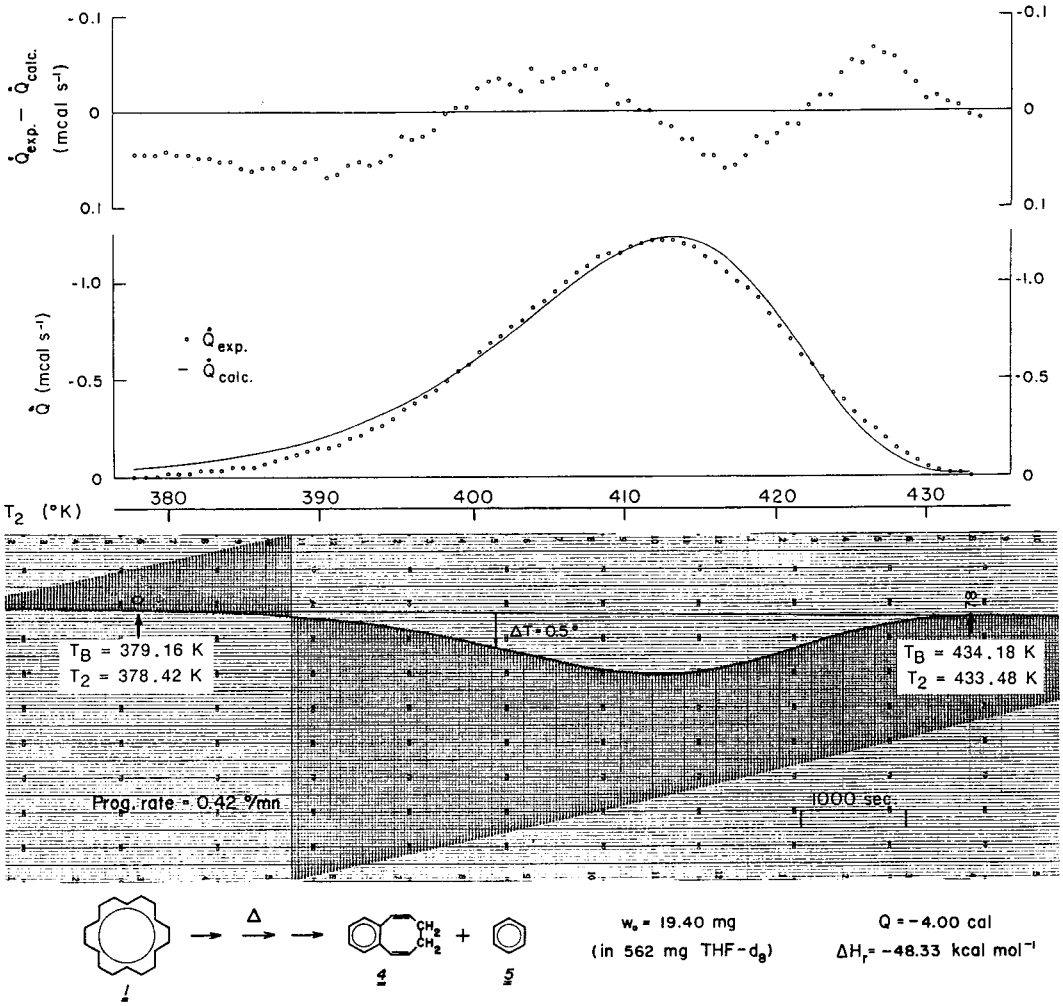


**Figure 2.** Experimental (105) and calculated thermograms for the thermolysis of [18]annulene. The iteratve calculations were performed assuming a single first-order reaction. The experimental recording displays both the linearly increasing block temperature and the temperature difference ($T_1 - T_2$) between the reference and sample cells as a function of time.

iterative computations using the program CALIT-2, assuming one single first-order reaction (Scheme 1). As can be seen in Figure 2, the errors $\dot{Q}_{exp} - \dot{Q}_{calc}$ are not statistically distributed; this indicates that the proposed kinetic mechanism (Scheme 1) is not correct.

**SCHEME 1**

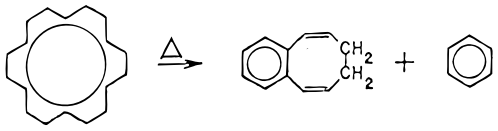

**1** **4** **5**

In order to elucidate the mechanism of the thermal transformation of **1** into **4** and **5**, we have followed, as a function of time, the composition of a solution of [18]annulene heated at 92 °C. The composition of the solution was deduced from the recorded $^1$H-NMR spectra; the concentrations of **1**, **4**, and **5** are reported, as function of time, in Figure 3.[3]

This figure shows that one (or more) intermediate(s) is (are) implicated in the thermal rearrangement, the maximum concentration of the intermediate(s) occuring after ca. 24 h thermolysis. In an independent experiment, we have isolated the intermediate(s) and could show that it corresponds to one or more tetracyclic structures **2** of molecular formula $C_{18}H_{18}$.[7] The $^1$H-NMR spectrum of the isolated intermediate(s) **2** as well as the spectrum of the hydrogenated product(s) are represented in Figure 4.[1,8]

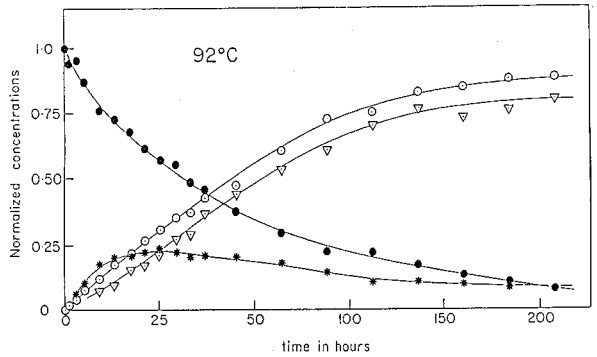


**Figure 3.** Concentration of the different compounds **1**, **2** + **3**, **4** and **5** present in the solution as a function of the time of thermolysis at 92 °C: ●, [18]annulene **1**; ▽, 1,2-benzo-1,3,7-cyclooctatriene **4**; ⊙, benzene; ∗, tetracyclic intermediates **2a**, **2b**, **2c** and *trans*-bicyclo-[6.4.0]dodeca-2,4,6,9,11-pentaene **3**.

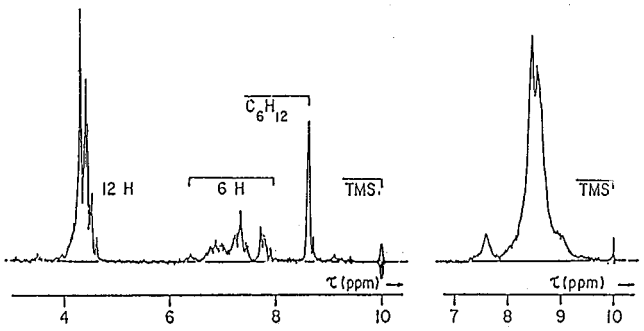


**Figure 4.** $^1$H-NMR spectra of the intermediate $C_{18}H_{18}$ tetracyclic compound(s) **2** (in cyclohexane-$d_{12}$, 100 MHz, 30 °C) and of its fully hydrogenated derivative(s) $C_{18}H_{30}$ (in benzene-$d_6$, 100 MHz, 30 °C).[10]

The intermediate compound(s) **2** must have one of the three possible structures **2a, 2b**, or **2c** (*c* = cis ring fusion; *t* = trans).

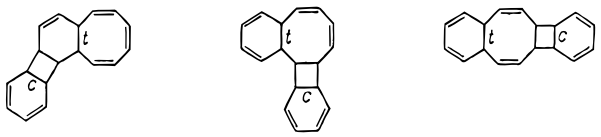

**2a** **2b** **2c**

These structures are the only ones compatible with the following observations:

(a) $^1$H-NMR spectrum (Figure 4) and decoupling experiments,[8] IR and MS spectra (molecular peak at *m/e* = 234);

(b) photochemical rearrangement of **2** carried out at −100 °C in THF-$d_8$ ($\lambda$ = 350 nm) gives benzene and [12]annulene;[6,7]

(c) catalytic hydrogenation of **2** indicates the presence of six double bonds in the molecule; the MS of the fully hydrogenated derivative(s) (molecular peak *m/e* = 246) indicates a tetracyclic saturated $C_{18}$-hydrocarbon.[7]

We have therefore simulated the thermograms using the CALIT-3 program, considering two succesive first-order reactions (rate constants $k_1$ and $k_2$) according to the reaction given in Scheme 2.

**SCHEME 2**

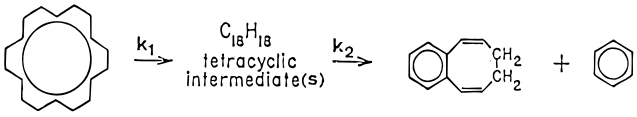


**1** **2** **4** **5**

According to these simulations, the total quadratic error

$$\text{tot. quad. error} = \sum_{\text{all points}} (\dot{Q}_{exp} - \dot{Q}_{calc})^2$$

resulting from the iterative calculations is smaller than the corresponding error as obtained from the iterative calculations assuming a single reaction. This can be seen from Table 2. Here also, as for the simulation assuming one single reaction, the errors $\dot{Q}_{exp} - \dot{Q}_{calc}$ are not statistically distributed, indicating that the kinetic approach is not yet satisfactory (see Figure 5).

We have therefore isomerized a solution of [18]annulene in THF-$d_8$ (in a sealed 5 mm NMR tube) at 92 °C and for 24 h, that is, under conditions where the concentration of the intermediate(s) should be the highest, and then recorded the $^1$H-

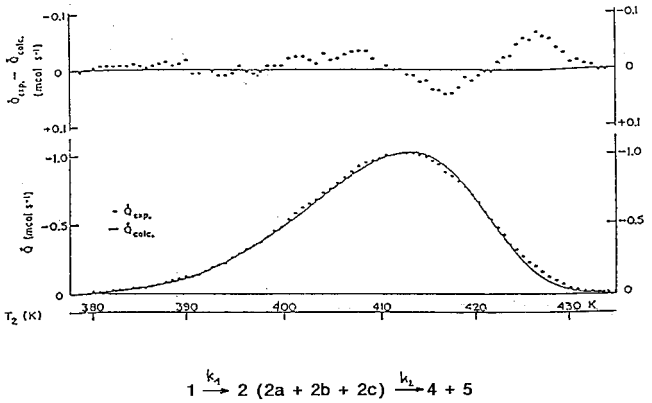


**Figure 5.** Simulation of thermogram 105 by iterative computations (CALIT-3) assuming two consecutive first-order reactions (Sheme 2). The errors distribution is not statistical.

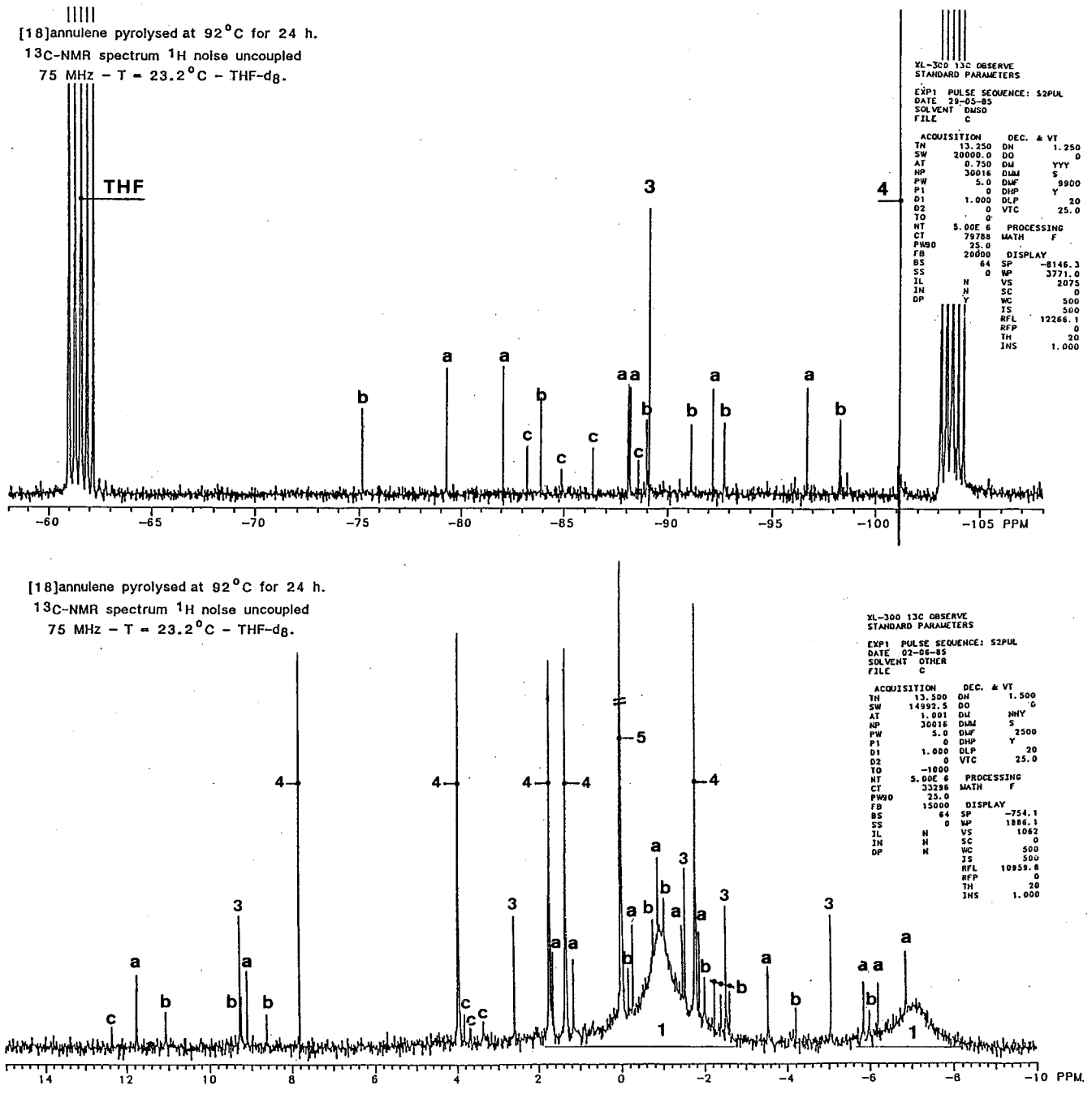


**Figure 6.** $^{1}$H noise decoupled $^{13}$C-NMR spectrum of a solution of [18]annulene in THF-$d_8$ thermolized at 92 °C during 24 h (Varian spectrometer XL-300, 75 MHz; lock signal, TMS-$d_{12}$; chemical shift reference ($\delta = 0$), $C_6H_6$; temperature, 23.2 °C). Top: Only the aliphatic region is represented here. Bottom: Only the olefinic region is represented here.

noise-decoupled $^{13}$C-NMR spectrum (at 30 °C). This spectrum, reproduced in Figure 6 (aliphatic domain and olefinic domain), clearly indicates that, next to quadricyclic intermediate compounds **2a**, **2b**, and **2c**, the precursor of **4**, i.e., *trans*-bicyclo-[6.4.0]dodeca-2,4,6,9,11-pentaene **3**, also accumulates in the reaction mixture.

This observation led us to modify our interpretation of the diagram represented in Figure 3; the data marked by * do not correspond to the concentration of **2** exclusively, but rather to **2** and **3** (the proton signals of these compounds are superposed). Furthermore, the fact that the curves marked by ⊙ (benzene **5**) and by ▽ (1,2-benzo-1,3,7-cyclooctatriene **4**) are still separated after 210 h reaction means that the reaction is not completed (**1** is still present) and is not due to polymerization of **4**, as we initially thought. Therefore, in the interpretation of the reaction heats, we do not introduce the corrections for polymerization of **4** as we have postulated and introduced in ref 1.

We have therefore simulated the thermograms with the CALIT-3 program,[3] considering three successive reactions according to the reaction in Scheme 3 in which the identification of the rate constants is the following:

$k_1$ for reaction **1** → **4** $k_2$ for reaction **2** → **3** + **5**

$k_3$ for reaction **3** → **4**

The simulation of the thermograms, after CALIT-3 iterative computations considering three consecutive reactions, gives optimal fit of the experimental data. The total quadratic error is smaller than those obtained considering only one (Scheme 1) or two reactions (Scheme 2) as indicated in

**SCHEME 3**

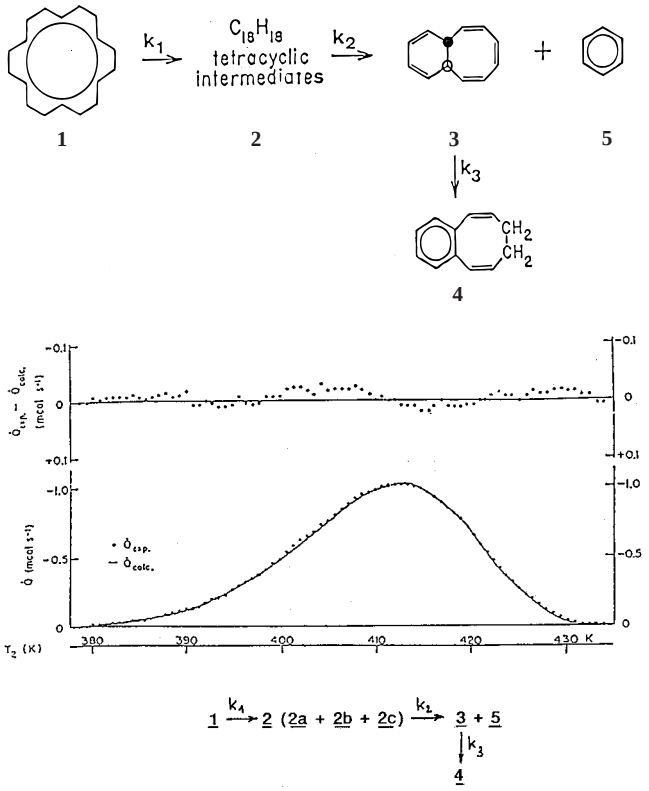


**Figure 7.** Simulation of thermogram 105 by iterative computations (CALIT-3) assuming three consecutive first-order reactions (Scheme 3). The errors distribution is statistical.

Table 2. The distribution of the errors $\dot{Q}_{exp} - \dot{Q}_{calc}$ is now statistical as shown in Figure 7; this indicates that the reaction mechanism adopted (Scheme 3) is the correct one.

The thermochemical and kinetic results of the analysis of the thermograms performed according to the mentioned mechanism (Scheme 3) are reported as tables below (Tables 3−6); their interpretation will be discussed.

### III. The Numerical Results of the Simulations of Thermograms 101, 104, and 105, the Computations Being Performed with the CALIT-3 Program, Three Consecutive Reactions Are Considered (Scheme 3)

The experimental conditions used for the investigation by scanning calorimetry of the thermal rearrangement of [18]-annulene **1** are listed in Table 1; three thermograms were measured.

Table 2 gives the total quadratic errors obtained after the the iterative simulations of the thermograms considering one reaction (Scheme 1), two reactions (Scheme 2) and, ultimately, three consecutive reactions (Scheme 3). This table displays the obvious improvement achieved in the quality of the fittings when considering three successive reactions.

In Table 3 we report, for each thermogram, the results of the measured total reaction heat ($Q_r$ tot), the total enthalpy change $\Delta_r H$(**1**, sol., 415 K) for the rearrangement of 1 mol of [18]annulene in solution, and the enthalpies changes of the three individual reactions.

The averaged values of these enthalpy changes are then reduced to standard conditions (i.e., 298.15 K and gas phase) and are reported in Table 4. The required enthalpies of sublimation and of vaporization[9] as well as the methods

**TABLE 1: Experimental Conditions of the Three Thermograms Recorded for the Thermal Rearrangement of [18]Annulene 1**

| | [18]annulene | | solvent | | progr. rate |
|---|---|---|---|---|---|
| run no. | $w_0$ (mg) | $n_0$ (mmol) | chemical | $w$ (mg) | $\dot{T}_B$ (deg/min) |
| 101 | 22.65 | 96.65 | toluene-$d_8$ | 550 | 0.532 |
| 104 | 18.57[a] | 79.24 | THF-$d_8$ | 441 | 0.532 |
| 105 | 19.40[a] | 82. 78 | THF-$d_8$ | 582 | 0. 423 |

[a] Freshly recrystallized sample.

employed to perform, the temperature corrections[10] are indicated below this table.

The Arrhenius parameters $E_a$ and log $A$ obtained from the analysis of the three thermograms and for each individual reaction are reported in Table 5. These parameters, averaged over the three thermograms, are utilized in Table 6 to calculate the entalpies, the entropies, and the free energies of activation of the individual reactions. These thermodynamical parameters are given for the standard temperature of 298.15 K, but the rate constants $k_i$ ($i$ = 1, 2, 3) are quoted for the temperature of 150 °C, that is, for the mean temperature of the thermograms.

### IV. Discussion of the Enthalpy Change for the Overall Reaction 1 → 4 + 5

**IVa. The Enthalpy of Formation of [18]Annulene 1 in the Gas Phase at 298.15 K.** The enthalpy of formation $\Delta H_f^\circ$(**1**, g, 298 K) of [18]annulene in the gas phase at 298.15 K can now be derived as

$$\Delta H_f^\circ(\mathbf{1}, \text{g}, 298\text{ K}) = \Delta H_f^\circ(\mathbf{4}, \text{g}, 298\text{ K}) + \Delta H_f^\circ(\mathbf{5}, \text{g}, 298\text{ K}) - \Delta_r H(1 \longrightarrow\!\!\!\!\!\rightarrow \mathbf{4} + \mathbf{5}, \text{g}, 298\text{ K})$$

The enthalpy of formation of benzene **5** is known; the recommended value[9] is

$$\Delta H_f^\circ(\mathbf{5}, \text{g}, 298\text{ K}) = 19.81 \pm 0.13 \text{ kcal mol}^{-1}$$

The enthalpy of formation $\Delta H_f^\circ$(**4**, g, 298 K) of 1,2-benzo-1,3,7-cyclooctatriene **4** can be estimated with confidence, resorting to the group increment methods.[10,11,12,13] The value adopted is $\Delta H_f^\circ$(**4**, g, 298 K) = 53.5 + 0.5 kcal mol$^{-1}$ (cf. Table 7).

The enthalpy of formation of [18]annulene **1** is then

$$\Delta H_f^\circ(\mathbf{1}, \text{g}, 298\text{ K}) = 50.05 + 19.81 + 53.5 = 123.4 + 3.7 \text{ kcal mol}^{-1}$$

This value is much larger than the one reported by Beezer et al.[14] deduced from heat of combustion measurements. The value reported, $\Delta H_f^\circ$(**1**, g, 298 K) = 67 + 6 kcal mol$^{-1}$, is certainly incorrect and much too small since oxidation of [18]annulene in the bomb prior to combustion is unavoidable; the heat of combustion of the oxidized annulene would then be much smaller than the "correct" value, and, therefore, the enthalpy of formation reported also should be much too small. The evaluation of the enthalpy of formation of [18]annulene $\Delta H_f^\circ$(**1**, g, 298 K) as well as the signification of the stabilization (resonance) and of the $\pi$-bonds delocalization energies are summarized in Figure 8.

**TABLE 2: Total Quadratic Error after the Iterative Simulation of the Thermograms Considering One, Two, or Three Consecutive Reactions**

| experiment no. | no. of exptl points | 1 reaction $\mathbf{1} \xrightarrow{k_1} \mathbf{4} + \mathbf{5}$ | 2 reactions $\mathbf{1} \xrightarrow{k_1} \mathbf{2} \xrightarrow{k_2} \mathbf{4} + \mathbf{5}$ | 3 consecutive reactions $\mathbf{1} \xrightarrow{k_1} \mathbf{2} \xrightarrow{k_2} \mathbf{3} + \mathbf{5} \xrightarrow{k_3} \mathbf{4} + \mathbf{5}$ |
|---|---|---|---|---|
| 101 | 70 | 0.1372 | 0.0626 | 0.0556 |
| 104 | 68 | 0.1451 | 0.0970 | 0.0832 |
| 105 | 79 | 0.1360 | 0.0517 | 0.0463 |

[a] The total quadratic error is calculated as tot. quadr. error $= \sum_{\text{all points}}(\dot{Q}_{\text{exp}} - \dot{Q}_{\text{calc}})^2$.

**TABLE 3: Molar Reaction Enthalpies of the Three Individual Reactions As Obtained by the Iterative Fitting (CALIT-3) of the Three Thermograms Considering Three Consecutive Reactions**

| run no. | $w_0$ (mg) [18]annul. | $w$ (mg) solvent | $Q_r$ tot (cal) | $\Delta_rH$(sol., 415 K) for each reaction indicated (in kcal mol$^{-1}$) $\mathbf{1} \rightarrow\rightarrow \mathbf{4} + \mathbf{5}$ | $\mathbf{1} \xrightarrow{k_1} \mathbf{2}$ | $\mathbf{2} \xrightarrow{k_2} \mathbf{3} + \mathbf{5}$ | $\mathbf{3} \xrightarrow{k_3} \mathbf{4}$ |
|---|---|---|---|---|---|---|---|
| 101 | 22.65 | 350[a] | −4.59 | −47.49 | −5.86 | −12.52 | −29.11 |
| 104 | 18.57[c] | 441[b] | −3.81 | −48.08 | −5.34 | −12.18 | −30.56 |
| 105 | 19.40[c] | 582[b] | −4.00 | −48.32 | −5.16 | −12.49 | −30.67 |
| average: | | | | −47.96 | −5.45 | −12.39 | −30.12 |
| statistical errors[d] | | | | ±0.60 | ±0.35 | ±0.30 | ±1.10 |

[a] Toluene-$d_8$. [b] Tetrahydrofuran-$d_8$. [c] Freshly recrystallized sample. [d] The statistical error on the mean value of three measurements is $2\bar{s} = 2[(n^2 - n)^{-1}\sum(\bar{x} - x_i)^2]^{1/2}$.

**TABLE 4: Enthalpies of the Three Consecutive Reactions Reduced to Standard Conditions (298.2 K, Gas Phase, in kcal mol$^{-1}$)**

| reaction | $\Delta_rH$(sol., 415 K) (kcal mol$^{-1}$) | correction vap. + subl. | $\Delta_rH$(g, 415 K) (kcal mol$^{-1}$) | temperature corrections | $\Delta_rH$(g, 298.2 K) (kcal mol$^{-1}$) |
|---|---|---|---|---|---|
| $\mathbf{1} \rightarrow \mathbf{2}$ | −5.45 ± 0.35 | 0.0 | −5.45 ± 0.35 | 1.50 | −3.95 ± 0.35 |
| $\mathbf{2} \rightarrow \mathbf{3} + \mathbf{5}$ | −12.39 ± 0.30 | −5.9 ± 2.5 | −18.29 ± 2.80 | 2.47 | −15.82 ± 2.80 |
| $\mathbf{3} \rightarrow \mathbf{4}$ | −30.12 ± 1.10 | 0.0 | −30.12 ± 1.10 | −0.16 | −30.28 ± 1.10 |
| $\mathbf{1} \rightarrow\rightarrow \mathbf{4} + \mathbf{5}$ | −47.96 ± 0.60 | −5.9 ± 2.5 | −53.86 ± 3.1 | 3.82 | −50.05 ± 3.1 |

$\Delta_{sub}H(\mathbf{1}) = 28 \pm 1.25$ kcal mol$^{-1}$
$\Delta_{sub}H(\mathbf{2}) = 28 \pm 1.25$ kcal mol$^{-1}$
$\Delta_{vap}H(\mathbf{3}) = 14 \pm 1.25$ kcal mol$^{-1}$
$\Delta_{vap}H(\mathbf{4}) = 14 \pm 1.25$ kcal mol$^{-1}$
$\Delta_{vap}H(\mathbf{5}) = 8.09 \pm 0.01$ kcal mol$^{-1}$

temperature corrections:
$\rightarrow \Delta_rH$(g, 298 K) $= \Delta_rH$(g, 415 K) − (415 − 298.2)$\Delta C_P$
$\Delta C_P = \sum C_P$(products) − $\sum C_P$(reagents) (the $C_P$ taken at 356 K)
$\rightarrow \Delta_rH$(g, 298 K) $= \Delta_rH$(g, 415 K) − $\sum\{(H^\circ_{415} - H^\circ_0) - (H^\circ_{298} - H^\circ_0)\}_{\text{prod.}} + \sum\{(H^\circ_{415} - H^\circ_0) - (H^\circ_{298} - H^\circ_0)\}_{\text{reag.}}$

**TABLE 5: Arrhenius Parameters Deduced from the Iterative Analyses of the Thermograms 101, 104, and 105, the Three Consecutive Reactions $\mathbf{1} \xrightarrow{k_1} \mathbf{2}$, $\mathbf{2} \xrightarrow{k_2} \mathbf{3} + \mathbf{5}$, and $\mathbf{3} \xrightarrow{k_3} \mathbf{4}$ Being Taken into Consideration**

| run no. | $w_0$ (mg) [18]annulene | no. of exptl points | $\dot{T}_B$ (K min$^{-1}$) | tot. quadr. errors | reaction $\mathbf{1} \xrightarrow{k_1} \mathbf{2}$ $E_a$ (kcal mol$^{-1}$) | log $A$ | reaction $\mathbf{2} \xrightarrow{k_2} \mathbf{3} + \mathbf{5}$ $E_a$ (kcal mol$^{-1}$) | log $A$ | reaction $\mathbf{3} \xrightarrow{k_3} \mathbf{4}$ $E_a$ (kcal mol$^{-1}$) | log $A$ |
|---|---|---|---|---|---|---|---|---|---|---|
| 101 | 22.65 | 70 | 0.532 | 0.0556 | 36.63 | 16.245 | 34.83 | 16.209 | 33.59 | 16.335 |
| 104 | 18.57 | 68 | 0.532 | 0.0832 | 36.62 | 16.268 | 34.61 | 16.309 | 33.22 | 16.317 |
| 105 | 19.40 | 79 | 0.423 | 0.0463 | 36.62 | 16.274 | 34.48 | 16.478 | 33.38 | 16.353 |
| mean values | | | | | 36.625 | 16.262 | 34.64 | 16.332 | 33.39 | 16.335 |
| statistical errors $2\bar{s} = 2[(n^2 - n)^{-1}\sum(\bar{x} - x_i)^2]^{1/2}$ | | | | | ±0.006 | ±0.017 | ±0.20 | ±0.157 | ±0.21 | ±0.020 |

**TABLE 6: Averaged Values of the Kinetic Parameters for Each of the Three Consecutive Reactions**

| reaction | $E_a$ (kcal mol$^{-1}$) | $\log_{10} A$ | $k_i$(150 °C) (s$^{-1}$) | values at 298.15 K $\Delta H^\ddagger$ (kcal mol$^{-1}$) | $\Delta S^\ddagger$ (cal mol$^{-1}$ K$^{-1}$) | $\Delta G^\ddagger$ (kcal mol$^{-1}$) |
|---|---|---|---|---|---|---|
| $\mathbf{1} \xrightarrow{k_1} \mathbf{2}$ | 36.625 ± 0.006 | 16.2624 ± 0.017 | $2.22 \times 10^{-3}$ | 36.03 ± 0.01 | 13.88 ± 0.08 | 31.89 ± 0.01 |
| $\mathbf{2} \xrightarrow{k_2} \mathbf{3} + \mathbf{5}$ | 34.64 ± 0.20 | 16.3317 ± 0.16 | $2.76 \times 10^{-2}$ | 34.05 ± 0.2 | 14.20 ± 1.0 | 29.82 ± 0.2 |
| $\mathbf{3} \xrightarrow{k_3} \mathbf{4}$ | 33.39 ± 0.21 | 16.3348 ± 0.020 | $1.23 \times 10^{-1}$ | 32.90 ± 0.21 | 14.22 ± 0.13 | 28.56 ± 0.21 |

**IVb. The Stabilization (Resonance) Energy of [18]Annulene. The Activation Enthalpy of the Conformational Mobility in [18]Annulene.** The stabilization energy due to the resonance in the $\pi$-system, according to the definition by Mortimer,[15] is the difference between the enthalpy of formation $\Delta H^\circ_f(\mathbf{1}, \text{g}, 298\text{ K})$ of [18]annulene (**1**, $D_{6h}$) and the enthalpy of formation $\Delta H^\circ_f(\mathbf{1k}, \text{g}, 298\text{ K})$ of the hypothetical planar Kékulé structure **1k** (symmetry $D_{3h}$) with alternating single and double bonds at their normal lengths.

$$\Delta H_{\text{stab}}(\mathbf{1}) = \Delta H^\circ_f(\mathbf{1}, \text{g}, 298\text{ K}) - \Delta H^\circ(\mathbf{1k}, \text{g}, 298\text{ K})$$

The enthalpy of formation of the hypothetical Kékulé annulene **1k** is readily calculated from thermochemical tables giving the enthalpy of formation of groups. The value adopted is (cf. Table 7)

$$\Delta H^\circ_f(\mathbf{1k}, \text{g}, 298\text{ K}) = 161 \pm 0.8\text{ kcal mol}^{-1}$$

The stabilization energy due to the resonance in the $\pi$-system of [18]annulene is therefore

$$\Delta H_{\text{stab}}(\mathbf{1}) = 123.4 - 161 = -37.6 \pm 4.5\text{ kcal mol}^{-1}$$

i.e., a value very close to the corresponding quantity found for benzene (−36.0).[15]

**TABLE 7: Estimation, Using Three Group Increment Methods, of the Enthalpy of Formation of the Different Compounds 4, 1k, 2 = ⟨2a, 2b, 2c⟩, 3 Implied in the Discussion of the Reaction Enthalpies of the Three Successive Reactions**

| | tables used | | | |
|---|---|---|---|---|
| | Franklin[10,11] | Wiberg[12] | Benson[13] | adopted value |
| benzocyclooctatriene **4** | 53.07 | 52.51 | 53.99 | 53.5 ± 0.5 |
| Kékulé [18]annulene **1k** | (163.62) | 161.4 | 160.62 | 161.0 ± 0.8 |
| tetracyclic intermediates **2** = (**2a** + **2b** + **2c**)/3 | 118.14 | 123.5 | 116.74 | 119.1 ± 3.0 |
| *trans*-bicyclopentaene **3** | 85.02[a] | 83.04[a] | 84.94 | 84.33 ± 1.2 |

[a] The stabilization energy in the plane *cis*−*s cis*−*cis*-butadiene (in cyclohexadiene) is taken as −3.5 kcal mol$^{-1}$, and in 1,3,5-cyclooctatriene as −3.7 kcal mol$^{-1}$ (value deduced from the heat of hydrogenation of COT[9] and from the comparison of the deduced enthalpy of formation of 1,3,5-cyclooctatriene with the value calculated by using the group increments methods).

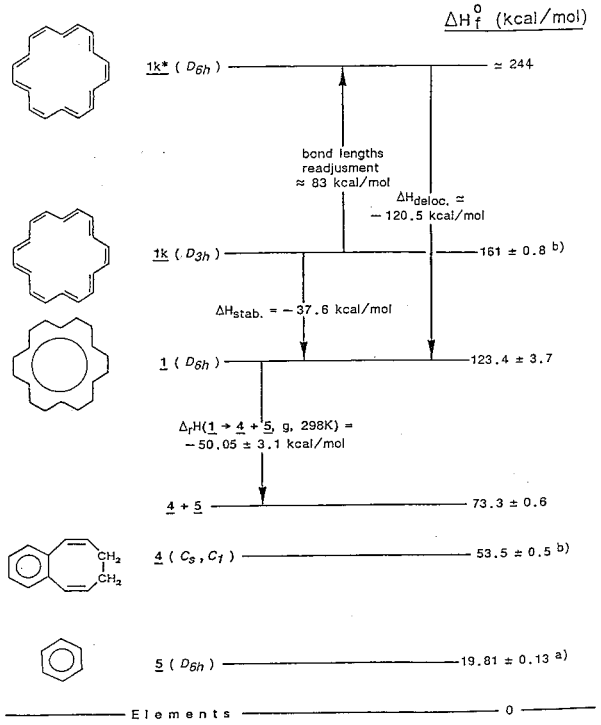


**Figure 8.** Determination of the enthalpy of formation $\Delta H_f^\circ$(**1**, g, 298.15 K) of [18]annulene and of its stabilization (resonance) and its $\pi$-bonds delocalization energies: (a) Cox and Pilcher;[9] (b) calculated values using group increment methods.[10−13]

Note that the Hückel resonance energy in [18]annulene (of symmetry $D_{18h}$) is equal to 5.35$\beta$ while in benzene it is equal to 2$\beta$.

We now have to explain why the activation enthalpy $\Delta H^\ddagger$ = 16.1 ± 0.2 kcal mol$^{-1}$ determined for the conformational mobility of the [18]annulene **1**[16−18] is much smaller than the absolute value of the stabilization energy, although the mechanism of this mobility implies that the cyclic delocalization of the $\pi$-bonds must be destroyed, since in the transition state three trans double bonds or three butadiene residues of configuration trans-s trans-trans must be perpendicular to the "mean" molecular plane[16] (the possible transition state structures for the conformational mobility in [18]annulene **1** are represented in Scheme 4). In fact each of the possible transition state structures contains three planar butadiene residues with a stabilization energy per residue of − 3.5 kcal mol$^{-1}$.[19]

The activation enthalpy for the conformational mobility should therefore be calculated as follows

$$\Delta H^\ddagger = |\Delta H_{stab}(\mathbf{1})| - 3|\Delta H_{stab}(C_4H_6)| = 37.6 - (3 \times 3.5) = 27 \pm 4.5 \text{ kcal mol}^{-1}$$

**SCHEME 4: Possible Structures of the Transition State Implied in the Conformational Mobility of [18]Annulene 1 with Their Symmetry Indicated**

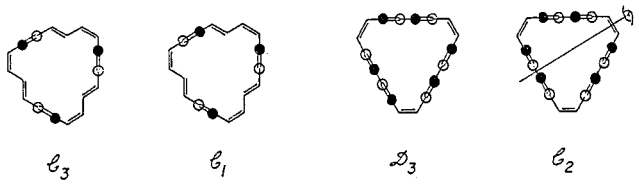


This estimation of the activation enthalpy for the conformational mobility in [18]annulene is **11** kcal larger than the experimental value $\Delta H^\ddagger$ = 16.1 kcal mol$^{-1}$. This implies either that only a part of the stabilization energy of [18]annulene **1** is lost along the conformational mobility pathway or that strain release effects have to be invoked. Indeed, we have also to consider that angular strain is present in [18jannulene **1** in order to relax the steric repulsion between the six inner protons (cf. X-ray data[20]); this strain disappears in the transition state structures, and this fact has also to contribute to the reduction of the activation enthalpy of the conformational mobility process.

**IVc. The $\pi$-Bond Delocalization Energy.** The delocalization energy $\Delta H_{deloc}$(**1**) in [18]annulene is the difference between the enthalpy of formation $\Delta H_f^\circ$(**1**, g, 298 K) of [18]annulene (**1**) and the enthalpy of formation $\Delta H_f^\circ$(**1k***, g, 298 K) of the hypothetical planar Kékulé structure **1k*** (symmetry $D_{6h}$) with localized single and double bonds having lengths identical to those in the real [18]annulene molecule **1**.

To calculate the enthalpy of formation of the Kékulé structure **1k*** ($D_{6h}$), we must therefore add to the estimated enthalpy of formation $\Delta H_f^\circ$(**1k**, g, 298 K) the energy required for the readjustment of the bond lengths as indicated here under

3 × $\sigma$-bond compression from 1.54 to 1.419 Å

6 × $\sigma$-bond compression from 1.54 to 1.382 Å

3 × double bond readjust from 1.34 to 1.419 Å

6 × double bond readjust from 1.34 to 1.382 Å

The bond lengths in [18]annulene **1** are known from an X-ray study[20] and are reported in Scheme 5 where [18]annulene **1** is represented together with the hypothetical Kékulé structures **1k** and **1k***. The relevant bond lengths and the point group of these species are indicated (note that only the geometry of the molecular skeleton is taken into account when considering the point group of **1k***; the $\pi$-bond distribution is not considered).

Using known force constants for the C−C bond in ethane and for the C=C bond in ethylene,[21] a total energy change of +83 kcal mol$^{-1}$ is calculated for these bond length readjust-

**SCHEME 5: Bond Lengths in [18]Annulene 1 and in the Hypothetical Structures 1k and 1k*[a]**

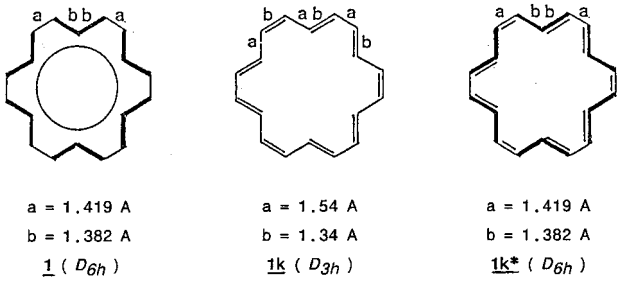


[a] The symmetry of the species is indicated.

ments. The estimated enthalpy of formation of the Kékulé [18]annulene **1k*** is then

$$\Delta H_f^\circ(\mathbf{1k^*}, \text{g}, 298\ \text{K}) \simeq 161 + 83 \simeq 244\ \text{kcal mol}^{-1}$$

and the $\pi$-bond delocalization energy in [18]annulene **1** is estimated to be (cf. Figure 8)

$$\Delta H_{\text{deloc}}(\text{bonds in } \mathbf{1}) = \Delta H_f^\circ(\mathbf{1}) - \Delta H_f^\circ(\mathbf{1k^*}) \simeq -120.5\ \text{kcal mol}^{-1}$$

Similar considerations concerning the benzene molecule give the following result:[15]

$$\Delta H_{\text{deloc}}(\text{bonds in } \mathbf{5}) = -63\ \text{kcal mol}^{-1}$$

**Remark.** If one considers the $\pi$-bond delocalization energy as identical to the Hückel resonance energy, and that the Hückel resonance energy in [18]annulene **1** is the same as in the annulene with $D_{18}$ perimeter, then we have the following determinations of the $\beta$ value:

benzene **5** $\quad 2\beta = -63\ \text{kcal mol}^{-1}$, i.e. $\beta = -31.5\ \text{kcal mol}^{-1}$

[18]annulene **1** $\quad 5.35\beta = -120.5\ \text{kcal mol}^{-1}$, i.e. $\beta = -22.5\ \text{kcal mol}^{-1}$

## V. Discussion of the Thermochemical and Kinetic Parameters of the Three Individual Consecutive Reactions

**Va. The Transformation of [18]Annulene 1 into the Quadricyclic Compounds 2a, 2b, and 2c.** These reactions can be explained formally by a series of successive or concomittant symmetry allowed intramolecular electrocyclizations. We will discuss the possible reaction pathways, their multipicity, and their stereochemical implications,[22] considering these electrocyclizations as consecutive reactions. We will consider the electronic structures of the two highest occupied molecular orbitals of [18]annulene calculated by the SCF−CNDO method. They are degenerate in energy and symmetry and are represented in Scheme 6.

The electrocyclization between two opposite centers such as 1−10 or 3−12 implying the cyclization of a 10 $\pi$-electron polyene must proceed thermally in a disrotatory fashion leading to a *cis* junction of the two rings formed, since the phases of the atomic orbitals of such opposite centers are in all cases identical and their H's are both pointing either inside or outside the ring. Such a process is practically excluded in view of the strain accumulated along the reaction pathway, as can be visualized from molecular model manipulations. On the contrary, the electrocyclization between centers such as 1−8 proceeding in a HMO's symmetry conservation fashion and leading to a cis junction between one 8-member ring and one 12-member ring, as well as the electrocyclization between centers such as 3−8 leading to a cis junction between one 6-member ring and one 14-member ring, are realistic processes. The multiplicity α (i.e., the number of identical or isodynamical[23] pathways) of each of these two types of ring closure is the following:

**SCHEME 6: The Two Degenerate (in Symmetry and in Energy) HOMO's of [18]Annulene (1) Calculated by the SCF-MNDO Method[a]**

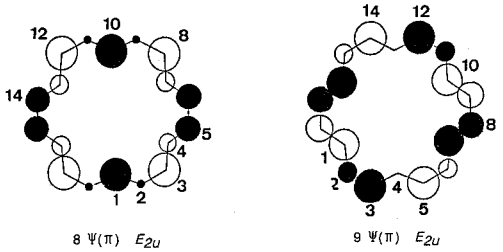


[a] The numeratation of the centers in the two HOMO's is chosen in order to avoid in the discussion the necessity to refer to different number identifications in the two orbitals.

ring closure of type 1−8 giving a cis ring fusion $\quad \alpha = 24$

ring closure of type 3−8 giving a cis ring fusion $\quad \alpha = 12$

*Note:* The value of the multiplicity of a reaction pathway α is found by direct counting of the identical ways of performing the reaction, or, better, by taking the ratio of the number of isometric[23] transition state structures to the number of isometric ground state structures:

$$\alpha = N_\ddagger / N_{\text{GS}}$$

These numbers $N$ ($N_\ddagger$ or $N_{\text{GS}}$) are calculated according to the following formula:

for an achiral species: $N = P/\sigma$

for a chiral species:[24] $N = 2P/\sigma$

in which $P$ is the dimension of the permutation group of Longuet−Higgins[25] (feasible permutations) and $\sigma$ the symmetry number of the species considered,[26,27] i.e., the number of distinct, physically feasible ways of orienting the species in space to give an indistinguishable configuration ($\sigma$ is the dimension of the subgroup of rotations of the point group characteristic of the species).

For the ring closure of type 1−8 giving a cis ring fusion, we have (cf. Scheme 7a)).

| ground state symmetry: $D_{6h}$ (achiral) | transition state symmetry: $C_1$ (chiral)[24] |
|---|---|
| symmetry number: $\sigma = 12$ | symmetry number: $\sigma = 1$ |
| permutation group dimension: $P = 2 \times 18$ | permutation group dimension: $P = 2 \times 18$ |
| $N_{\text{GS}} = (2 \times 18)/12 = 3$ | $N_\ddagger = (2 \times 2 \times 18)/1 = 72$ |

The reaction path multiplicity is then $\alpha = N_\ddagger/N_{\text{GS}} = {}^{72}/_3 = 24$.

For the ring closure of type 3−8 giving a cis ring fusion, we have (cf. Scheme 7b)

| | |
|---|---|
| ground state symmetry: $D_{6h}$ (achiral) | transition state symmetry: $C_s$ (achiral) |
| symmetry number: $\sigma = 12$ | symmetry number: $\sigma = 1$ |
| permutation group dimension: $P = 2 \times 18$ | permutation group dimension: $P = 2 \times 18$ |
| $N_{GS} = (2 \times 18)/12 = 3$ | $N_{\ddagger} = (2 \times 18)/1 = 36$ |

The reaction path multiplicity is then $\alpha = N_{\ddagger}/N_{GS} = {}^{36}/_{3} = 12$.

**SCHEME 7: Symmetry of Possible Structures along the Reaction Path toward the Transition States for the Two Types of Electrocyclization of [18]Annulene 1 Discussed**[a]

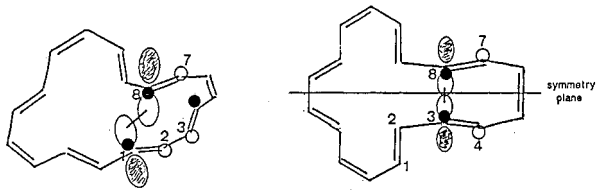


a) joining $C^1$ to $C^8$ giving a *cis* fusion of a 8 member and a 12 member rings
Symmetry $C_1$ - chiral - $\sigma$ = 1

b) joining $C^3$ to $C^8$ giving a *cis* fusion of a 6 member and a 14 member rings
Symmetry $C_s$ - achiral - $\sigma$ = 1

[a] The conformations of the 12-member ring and of the 14-member ring are not correctly represented; the planar structures are represented in order to emphasize their configurations.

The other ring closure steps leading to the tetracyclic compounds **2a**, **2b**, and **2c** are illustrated in Figure 9. It can be seen, using molecular models, that the formation of **2a**, and **2b** is easier than the formation of **2c**, the strain required to form the last rings in **2c** being greatest and the reaction path multiplicity being reduced in this last case. This explains why the relative abundances of **2a** and of **2b** are greater than that of **2c** (cf. Figure 6; note that in these figures the signals marked **a** designate signals of **2a** or **2b**, and the **b** signals designate compound **2b** or **2a**). One can also realize that the number of $^{13}$C-NMR olefinic signals marked **c** for **2c** is not 12 but smaller: the molecule has local symmetry such that 6 olefinic C atoms have pairwise the same chemical shift giving 3 signals with double the intensity of the 6 other olefinic C atoms; the 6 aliphatic C atoms give 4 $^{13}$C-NMR signals with relative intensities 2:2:1:1 for the same reason.

It is interesting that the multiplicity of the overall reaction **1** → **2a**, **2b**, and **2c** is responsible for a large part of the reported activation entropy $\Delta S^{\ddagger} = 13.88$ eu. If one assumes that all the ring closures are concomitant, the contribution of the multiplicity to $\Delta S^{\ddagger}$ is estimated to be $R \ln(48 + 48 + 24) = 9.51$ eu (cf. Figure 9). If the different ring closures implicated in the formation of the compounds **2a**, **2b**, and **2c** are not concomitant, intermediates are implied and the interpretation of the activation entropy of the reaction **1** → **2** in terms of reaction path multiplicity would have to be revised; the coefficients of transmission through the different barriers would have to be taken into account.

*The Reaction Enthalpy* $\Delta_r H$(**1** → **2a** + **2b** + **2c**, g, 298 K). The concentrations of compounds **2a**, **2b**, and **2c** being controlled kinetically and not thermodynamically, we will calculate, by group increment methods, the enthalpies of formation of the three compounds and consider the average of these values as representative of the enthalpy of formation of **2** (cf. Table 7). The adopted value for the enthalpy of formation of **2** is, in these conditions

$$\Delta H_f^{\circ}(\mathbf{2}, \text{g}, 298\ \text{K}) = 119.1 \pm 3.0\ \text{kcal mol}^{-1}$$

In view of the difficulties encountered in these calculations such as the estimation of the contribution of adjacent aliphatic CH groups and of the conjugation effects between double bonds, this adopted value is somewhat uncertain.

The calculated reaction enthalpy, using this value

$$\Delta_r H(\mathbf{1} \rightarrow \mathbf{2}, \text{g}, 298\ \text{K}) = \Delta H_f^{\circ}(\mathbf{2}, \text{g}, 298\ \text{K}) - \Delta H_f^{\circ}(\mathbf{1}, \text{g}, 298\ \text{K}) = 119.1 - 123.4 = -4.3\ \text{kcal mol}^{-1}$$

is, however, in excellent agreement with the experimental reaction enthalpy reported in Table 4:

$$\Delta_r H(\mathbf{1} \rightarrow \mathbf{2}, \text{g}, 298\ \text{K}) = -3.95\ \text{kcal mol}^{-1}$$

These considerations constitute a further support for the validity of the reported value for the enthalpy of formation of [18]-annulene **1**.

**Vb. The Decomposition of the Tetracyclic Compounds 2a, 2b, and 2c to Benzene 5 and *trans*-Bicyclopentaene 3.**[28] Each of the structures **2a**, **2b**, and **2c** contains a four-membered ring fused in cis fashion to a cyclohexadiene residue. Such a system decomposes thermally via a biradical that is stabilized by conjugation with the double bonds connected to the four membered ring. The activation enthalpy of this ring opening is easily estimated by considering the activation enthalpy of the decomposition of cyclobutane to two ethylenes ($E_a = 62.5$ kcal mol$^{-1}$, $\Delta H^{\ddagger} = 61.9$ [29]) and the stabilization enthalpy of the allyl radical ($\Delta H_{stab} = -13.5$ [30]). If two allyl (or allyl and pentadienyl) resonance energies are gained in the biradical, then the activation enthalpy of the C4-ring opening would be

$$\Delta H^{\ddagger}(\mathbf{2} \rightarrow \text{biradical}) = 61.9 - (\mathbf{2} \times 13.5) = 34.9\ \text{kcal mol}^{-1}$$

This value is in very good agreement with the observed enthalpy of activation of the reaction **2** → **3** + **5** reported in Table 6. This agreement implies that the biradical is in fact the transition state, or close to it, along the reaction path and that the splitting of benzene **5** takes place along the second part of the reaction path with continuous energy decay toward benzene **5** and *trans*-bicyclopentaene **3.**

The entropy of activation of the reaction is large, as is also the case for the activation entropy of the reaction, of 1,2-*cis*-dimethylcyclobutane giving two propene molecules ($\Delta S^{\ddagger} = 10.9$ eu at 298 K[29]). This is explained by the appearance of torsion modes of vibration around the residual C−C bond of the previous $C_4$ ring. For the reaction **2** → **3** + **5** discussed here, the value $\Delta S^{\ddagger} = 14.2 \pm 1$ eu is larger than 11 eu; this could mean that, in the biradical, the C−C bond is already weakened and has a lower stretching frequency than in the transition state for the decomposition of 1,2-*cis*-dimethylcyclobutane in two propene molecules.

*The Reaction Enthalpy* $\Delta_r H$(**2** → 3 + **5**, g, 298 K). The enthalpy change associated with the reaction **2** → **3** + **5** can be estimated as

$$\Delta_r H(\mathbf{2} \rightarrow \mathbf{3} + \mathbf{5}, \text{g}, 298\ \text{K}) = \Delta H_f^{\circ}(\mathbf{5}, \text{g}, 298\ \text{K}) + \Delta H_f^{\circ}(\mathbf{3}, \text{g}, 298\ \text{K}) - \Delta H_f^{\circ}(\mathbf{2}, \text{g}, 298\ \text{K})$$

The enthapies of formation of **5** and of **2** are known (see section V.a) and the enthalpy of formation of **3** is estimated by the group increments methods (cf. Table 7). One obtains

$$\Delta_r H(\mathbf{2} \rightarrow \mathbf{3} + \mathbf{5}, \text{g}, 298\ \text{K}) = 84.33 + 19.81 - 119.1 = -14.96\ \text{kcal mol}^{-1}$$

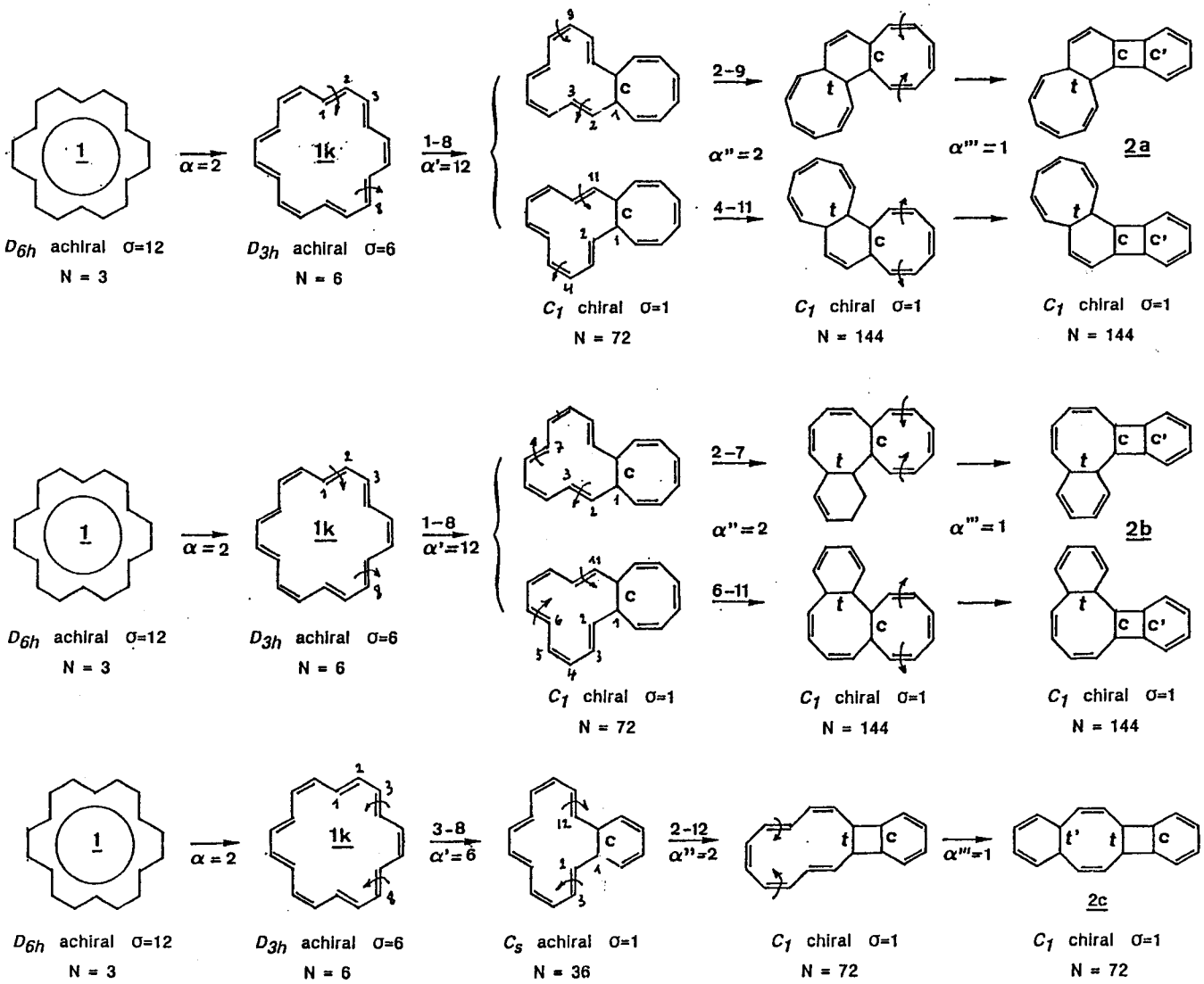


**Figure 9.** Hypothetic mechanisms proposed in order to establish the stereochemistry of **2a**, **2b**, and **2c** and to determine the multiplicity of the different rearrangements. If the ring fusions leading to each of compounds **2a**, **2b**, or **2c** are concomitant, then we have the following reaction path multipicities: **1** → **2a** $\alpha = 48$, **1** → **2b** $\alpha = 48$, **1** → **2c** $\alpha = 24$, i.e., overall **1** → **2** $\alpha = 120$. The contribution of the multiplicities to the activation entropy is $R \ln 120 = 9.51$ eu.

a value in perfect agreement with the experimental result reported in Table 4:

$$\Delta_f H(\mathbf{2} \rightarrow \mathbf{3} + \mathbf{5}, \text{g}, 298\ \text{K}) = -15.82 \pm 2.8\ \text{kcal mol}^{-1}$$

**Vc. The Transformation of *trans*-Bicyclopentaene 3 in Benzocyclooctatriene 4 as the Result of Two Consecutive Suprafacial 1,5-Hydrogen Shifts.** In our studies on the [12]-annulene,[5] the thermal rearrangement **3** → **4** was also studied using the first version of our scanning differential calorimeter.[31] The reaction was not found to be perfectly reproducible and was recognized to be sensitive to traces of water (acid-catalyzed reaction). Reproducible thermograms could finally be obtained by treating the Pyrex ampule with $NH_3$ vapor and using deuterated pyridine as solvent. The reaction was found to be first order, and no intermediate such as bicyclo[6.4.0]dodeca-1,3,6,9,11-pentaene **3a** could be detected.[6,32] All the parameters (thermochemical and kinetic) found for this reaction and reported in the present work (Tables 4 and 6) are in perfect accord with those deduced from these earlier measurements.

To obtain a better understanding of the mechanism of this reaction, we have established the reaction energy hypersurface,

**SCHEME 8: Choice of the Reaction Coordinates To Establish the Energy Hypersurface Computed in View of the Elucidation of the Mechanism of the Reaction 3 → 4**

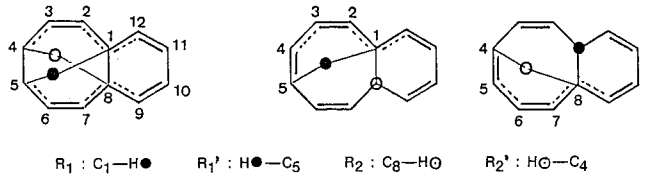


the reaction coordinates chosen being indicated in Scheme 8. The geometries have been optimized for all the values chosen for these parameters.[32] The computations were done, using a modified version of the program MOPN[33] that treats closed-shell molecules by the SCF−UHF method.[34] Since the UHF determinant is not an eigenfunction of the $S^2$ operator but reflects a mixture of different spin states, spin-annihilation[35] or spin-projection[36] techniques have been applied. The energy hypersurface is reproduced in Figure 10.

According to these computations, the two hydrogen shifts are not taking place synchronously but rather consecutively. The

**TABLE 8: Enthalpy of Formation $\Delta H_f^\circ$(g, 298 K) of the Species 3, 3a, 4 and of the Transition States $TS_{direct}$, $TS_1$, and $TS_2$ with the Geometries Found in the Computed Hypersurface[c]**

| | | | $\Delta H_f^\circ$ (kcal mol$^{-1}$) | | |
|---|---|---|---|---|---|
| species | state | symmetry | experiment | group incr. | UHF-MINDO-3 spin projection |
| **3** | G.S. | $C_1$ | $83.78 \pm 1.6$[a] | $84.33 \pm 1.2$ | 83.3 |
| **3** | strained | $C_2$ | | $87.4 \pm 2.5$ | |
| **3a** | G.S. | $C_1$ | | $81.4 \pm 1.3$ | 79.2 |
| **4** | G.S. | $C_s$ | | $53.5 \pm 0.5$ | 57.6 |
| **4** | strained | $C_2$ | | $57.9 \pm 1.5$ | 59.4 |
| $TS_{direct}$ | ‡ (**3** → **4**) | $C_2$ | | | 182.7 |
| $TS_1$ | ‡(**3** → **3a**) | $C_1$ | $116.7 \pm 1.8$[b] | | 127.8 |
| $TS_2$ | ‡(**3a** → **4**) | $C_1$ | | | 112.3 |

[a] Value found from the enthalpy of the reaction $\Delta_r H$(**3** → **4**, g, 298 K) = $-30.28 \pm 1.1$ and from the enthalpy of formation $\Delta H_f^\circ$(**4**, g, 298 K) = $53.5 \pm 0.5$ kcal mol$^{-1}$ calculated by the group increments methods (cf. Table 7). [b] $\Delta H_f^\circ(TS_1, 298\ K) = \Delta H_f^\circ$(**4**, g, 298 K) − $\Delta_r H$(**3** → **4**), g, 298 K) + $\Delta H^\ddagger(k_3, 298\ K) = 116.7 \pm 1.8$ kcal mol$^{-1}$. [c] For species **3** and **4** a second geometry is reported that is discussed in the text.

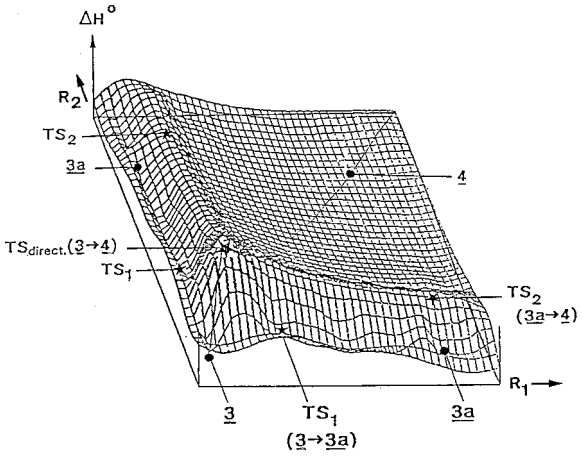


**Figure 10.** Potential energy surface computed in order to elucidate the mechanism of the double 1−5 hydrogen shift in *trans*-bicyclo-[6.4.0]dodeca-2,4,6,9,11-pentaene **3** giving 1,2-benzo-1,3,7-cyclooctatriene **4**. The diagonal **3** → $TS_{direct}$ → **4** corresponds to the synchronous shift of the two hydrogen atoms; the two off-diagonal paths **3** → $TS_1$ → **3a** → $TS_2$ → **4** represents the asynchronous mechanism (multiplicity 2).

implicated intermediate bicyclo[6.4.0]dodeca-1,3,6,9,11-pentaene **3a** is not observed since the activation enthalpy for the last reaction step **3a** → **4** is lower than the one of the first step. The enthalpies of formation of the species **3**, **3a**, and **4**, observed and computed, as well as the relevant activation enthalpies, are reported in Table 8.

Dewar has considered the abstract possibility of synchronous multibond-breaking reactions and has formulated the requirements for such mechanisms to occur.[37] According to his arguments, synchronous hydrogen shifts would be favored if three conditions were satisfied:

(i) the transition state has to be aromatic;

(ii) the reaction has to be exothermic;

(iii) the amount of strain relieved in the transition state has to be larger for the synchronous than for the asynchronous pathway.

The first condition is by far verified if one considers the double H shift to occur in the $C_2$ conformation of **3** since, upon breaking the two C−H bonds, the $\pi$-system of benzene is formed. The strain accumulated in the $C_2$ conformation of **3** should be relatively small; in fact this $C_2$ conformation corresponds to the transition state of the isodynamic transformation of **3** ($C_1$) into itself (inversion of the cyclooctatriene ring) with retention of the absolute configuration. The energy cost for this ring inversion is smaller than the 11 kcal mol$^{-1}$ required for the inversion of cyclooctatetraene[17] since here the resonance energy in the quasi-planar triene is gained. The estimation of $\Delta H_f^\circ[\mathbf{3}(C_2)] - \Delta H_f^\circ[\mathbf{3}(C_1)]$ amounts to 3−4 kcal mol$^{-1}$. The synchronous shift of the two hydrogen atoms would occur in this conformation, the $C_2$ symmetry axis remaining preserved in the complete dynamic process as well as in the product **4**, which would then relax in the achiral $C_s$ geometry.

The second condition is clearly verified, the reaction enthalpy being equal to

$$\Delta_r H(\mathbf{3} \rightarrow \mathbf{4}) = -30.28 \text{ kcal mol}^{-1}$$

The third condition is not fulfilled, although the strain accumulated in the $C_2$ conformation of $TS_{direct}$ is only slightly larger than in the transition states $TS_1$ and $TS_2$ with the $C_1$ conformations.

The occurrence of synchronous two-bond-breaking in chemical processes is unlikely; accumulating the energy required to break two bonds specifically in two vibrational modes prior to energy redistribution to all the other degrees of freedom of the molecule is hardly possible.

Let us now interpret the high positive value of the activation entropy of the reaction **3** → **4** $\Delta S^\ddagger = 14.22 \pm 0.13$ eu. For each enantiomer of **3** ($C_1$ symmetry), there are two isodynamic pathways for the 1−5 H-shift process, i.e., a contribution of $R\cdot\ln 2 = 1.38$ eu to the entropy of activation. But the most important contribution to the activation entropy is due to the motion of the migrating H atom; this motion accounted as a translation mode along one coordinate contributes to the entropy of activation by a quantity of 8.67 eu. Taking into account the multiplicity $\alpha = 2$, the total contribution amounts to 10.05 eu. Note that for the synchronous mechanism, the contribution to the activation entropy of the simultaneous translation of the two H's would be 17.34 eu.

We can now construct the full diagram representing the enthalpy evolution when going from **1** to **4** + **5** along the reaction pathways discussed (Figure 11).

## VI. Verification of the Validity of the Kinetic Data Gained from the Reported Analysis of the Thermograms

**VIa. Direct Measurement of the Kinetic Parameters of the First Reaction 1 → 2.** We have followed, by UV spectroscopy, the isothermal disappearance of [18]annulene as a function of time at seven different temperatures (between 90 and 150 °C). The measurements were done by warming the solution of annulene at constant temperature (oil bath) for controlled periods of time in a UV cell specifically constructed so that the solution could be degassed under high vacuum and the cell sealed off. In order to optimize the experimental conditions, we had to find the concentration of annulene to be

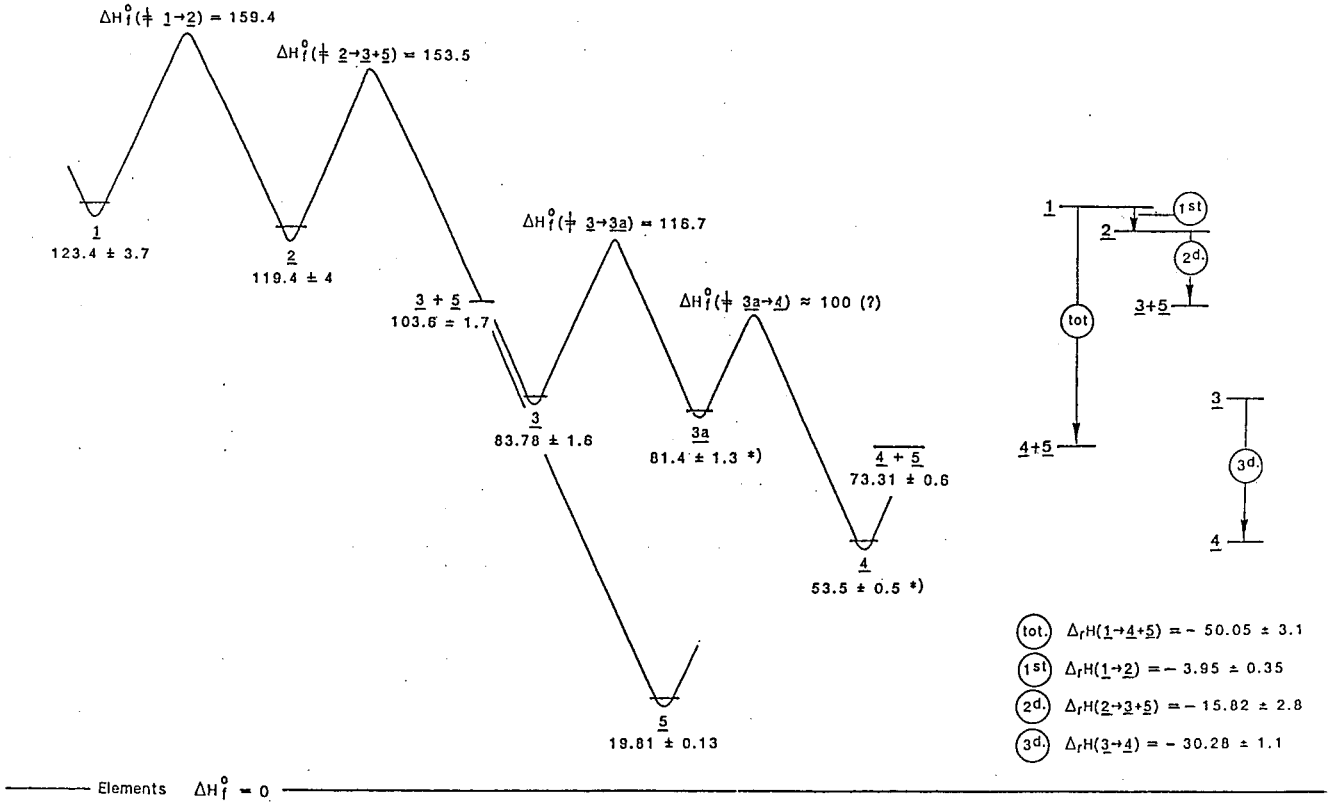


**Figure 11.** Enthalpies of formation of all the species involved in the thermal rearrangement of [18]annulene **1** into benzene **5** and 1,2-benzo-1,3,7-cyclooctatriene **4** and of all the transition states implied by the three consecutive first-order reactions. All values are in kcal mol$^{-1}$. Only the enthalpies of formation of **4** and **3a** (marked by *) are calculated by the group incement methods; all the other data are measured.

used, the optical path to be chosen for the cell, and the absorption band of the annulene to be measured in order to monitor the kinetic experiments. For these reasons, a preliminary thermolysis experiment was conducted at 120 °C using cells with different optical paths. The results are reported in Figure 12.

A cell with an optical path of 0.02 cm was chosen in order to work with the realistic concentration of 7.04 mg of [18lannulene in 100 mL of THF. i.e., $3.0 \times 10^{-4}$ mol L$^{-1}$. The optical density of the absorption band at $\lambda = 384$ nm measured at −100 °C on this stock solution is OD = 1.75, a suitable value in order to follow the disappearance of the annulene since the absorption at this wavelength due to the reaction products is negligible (OD ≃ 0). The measurements were performed by quenching the cell in a dry ice−methanol bath (−80 °C) after each time of thermolysis and transferring the cell in a gas flow cryostat with sapphire windows, the temperature of which was controlled and maintained at −100 °C. The UV spectrometer is a Cary 17, modified in order to digitize the wavelengths and the OD data and to transfer them to a desktop computer.

The rate constants $k_T$ were found by the linear regression of the measured values of $\log[(OD_0 - OD_t)/OD_0]_t$ obtained at different times. Finally the linear regression of log $k_T$ as a function of 1000/$T$ gave the following Arrhenius and thermodynamic parameters:

$$E_a = 35.9 \pm 0.2 \text{ kcal mol}^{-1} \qquad \log A = 16.03 \pm 0.2 \text{ eu}$$

$$k_1(150\ ^\circ\text{C}) = 3.10 \times 10^{-3}\ \text{s-1}$$

$$\Delta H^{\ddagger} = 35.3 \pm 0.5 \text{ kcal mol}^{-1} \qquad \Delta S^{\ddagger} = 12.8 \pm 0.8 \text{ eu}$$

$$\Delta G^{\ddagger} = 31.6 \pm 0.5 \text{ kcal mol}^{-1}$$

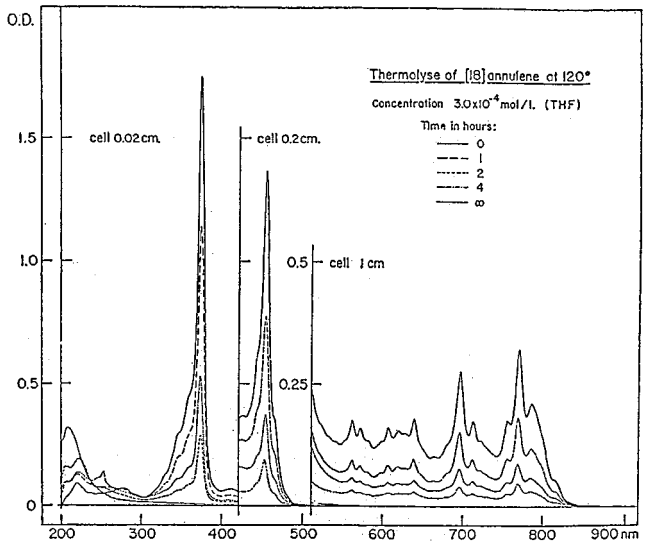


**Figure 12.** Preliminary measure of the rate of disappearance of [18]-annulene at 120 °C. This measure was carried out in order to optimize the experimental conditions of the kinetic studies observed by UV spectroscopy.

which are in very good agreement with the results reported in Table 6 (reaction **1** → **2** ).

The Arrhenius regression line of these UV kinetic measurements is represented (with the data points) in Figure 13, together with the individual regression lines for the kinetic results for the three processes $k_1$, $k_2$, and $k_3$ as obtained from the thermogram analysis. Also are represented, in this figure, the rate constants $k_1(T)$ at two temperatures deduced from two kinetic measurements performed by $^1$H-NMR spectroscopy.

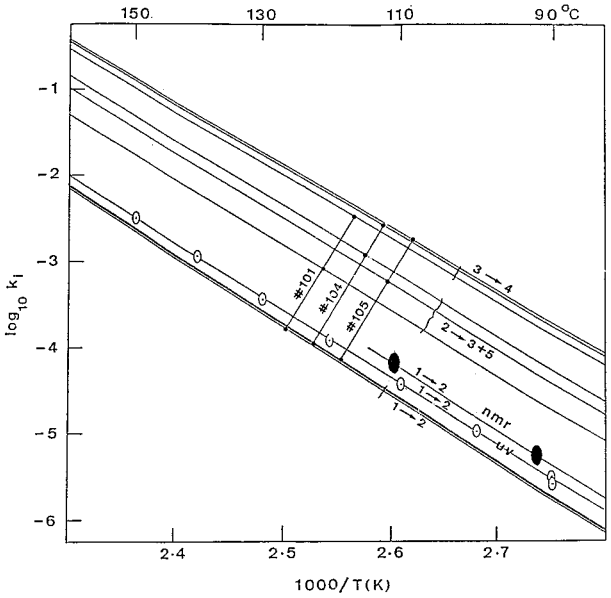


**Figure 13.** Regression lines according to the Arrhenius equation of the kinetic data for the reaction $\mathbf{1} \xrightarrow{k_1} \mathbf{2}$ studied by UV spectroscopy (the data points are represented) and of the data for the three consecutive reactions, as obtained from the iterative simulations of the three thermograms (the data points are not represented here). Two data points, deduced from $^1$H-NMR measurements, are also represented.

This figure emphasizes the fact that the Arrhenius regressions lines for the reactions $\mathbf{1} \xrightarrow{k_1} \mathbf{2}$ and $\mathbf{3} \xrightarrow{k_3} \mathbf{4}$ are reproducible in the three thermograms, the regression lines for the reaction $\mathbf{2} \xrightarrow{k_2} \mathbf{3} + \mathbf{5}$ differing somewhat from one thermogram to the other. This situation is demonstrated in Table 5, which shows that the frequency factor for this second reaction is the least precisely determined of all the kinetic parameters.

**VIb. The Relative Concentrations of the Species 1, 2 (2a + 2b + 2c), 3, 4, and 5 as Functions of the Temperature (or Time) in the Course of the Measurement of a Thermogram.** In the iterative process, controlled by the CALIT-3 program, when the iteration is stopped i.e., when the total quadratic error has reached its minimum value, the kinetic parameters of the last iteration step are utilized to compute the evolution of the relative concentration of each component present in the solution (in mole fraction) as a function of the temperature (or of the time) defined by the thermogram. These data are plotted in graphic form as part of the computer output. Figure 14 represents the graph giving the evolution of the composition of the solution during its thermolysis in the calorimeter (thermogram 105) as obtained at the end of the iterative computations.

With the aid of this graph, a very effective test of the validity of the analysis of the thermograms could be envisaged: a new calorimetric run with controlled amounts of [18]annulene + solvent and with the same rate of temperature increase would have to be started but should be stopped when a precise temperatue, say 405 K (see Figure 14), would be reached. The cell containing the ampule should be immediately quenched in liquid nitrogen (the construction of the calorimeter easily allows such a manipulation) and the solution in the ampule directly analyzed by $^{13}$C-NMR spectroscopy. The mole fractions of the different components would have to be measured and compared to their values read on the graph (Figure 14) for the temperature at which the thermogram was stopped. Unfortunately we could not perform this ideal test, for the reason that we did not have enough material to invest 20 mg in such an experiment.

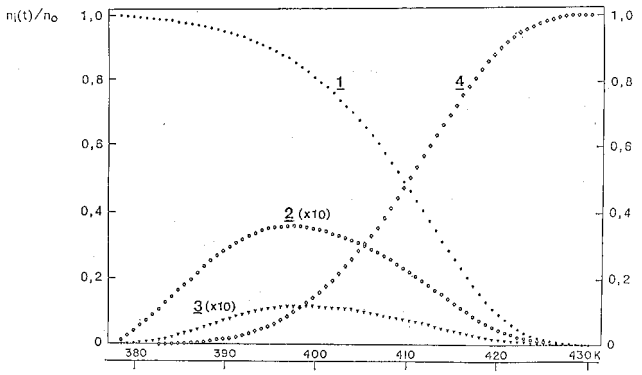


**Figure 14.** Mole fractions of compounds **1**, **2**, **3**, and **4** as functions of the temperature (or of time) as they are calculated and plotted after the iterative simulation (CALIT-3) of the 105 thermogram. The mole fraction of compound **5** is the sum of the mole fractions of **3** and **4**.

A somewhat related test could be made by close inspection of the $^1$H noise decoupled $^{13}$C-NMR spectra recorded for a solution of [18]annulene in THF-$d_8$ thermolyzed 24 h at 92 °C (spectrum reported on Figure 6). We have to compare the mole fractions of the constituents extracted from the spectra with those computed with the kinetic parameters reported for each thermogram in Table 5. This procedure allows us to avoid the problem of the correlation between $E_a$ and log $A$ in determining the average values and the dispersions of the rate constants and of the mole fractions.

According to the data of Table 5, we have, for the rate constants at 92 °C

$$k_1 = (2.20 \pm 0.11) \times 10^{-6}\ \mathrm{s}^{-1}$$

$$k_2 = (4.4 \pm 2.5) \times 10^{-5}\ \mathrm{s}^{-1}$$

$$k_3 = (2.25 \pm 0.75) \times 10^{-4}\ \mathrm{s}^{-1}$$

and, at each reaction time

$$n_1 + n_2 + n_3 + n_4 = n_0 \qquad n_5 = n_3 + n_4$$

$n_0$ is the number of moles of [18]annulene **1** introduced into the ampule.

The integration of the kinetic equations gives formulae that permit the calculation of the mole fractions of the different components after a given time of pyrolysis at a specified temperature (see section VIII below for the derivation and the integration of the kinetic equations).

For 24 h of pyrolysis at 92 °C, we calculate the following mole fractions of the different components:

$$n_1/n_0 = 0.827 \pm 0.007 \qquad n_2/n_0 = 0.048 \pm 0.021$$

$$n_3/n_0 = 0.0081 \pm 0.0012 \qquad n_4/n_0 = 0.117 \pm 0.027$$

$$n_5/n_0 = 0.125 \pm 0.027$$

In order to compare these calculated mole fractions with experimental data, the intensities (i.e., heights) of the $^{13}$C-NMR signals were measured on the original spectra. All the signals due to a given species have been added; this total was converted, by division by a suitable factor taking into account the number of different magnetic sites in the species and its symmetry, to obtain a quantity proportional to the number of moles of the species considered. This was done separately for the signals in the olefinic and in the alphatic regions. For each region, a

normalization procedure such that the mole fraction $n_5/n_0$ takes the computed value was adopted. This amounts to a coherent estimation of the number of moles $n_0$ of the [18]annulene involved in the thermolysis. This normalization number is different for the two regions, since the corresponding spectra are recorded with different sensitivity conditions. The results obtained are the following:

| olefinic domain | | aliphatic domain | |
|---|---|---|---|
| $n_2{}^a = 540/12 = 45$ | $n_2/n_0 = 0.0452$ | $n_2{}^a = 678/6 = 113$ | $n_2/n_0 = 0.0435$ |
| $n_3 = 250/(2\times5) = 25$ | $n_3/n_0 = 0.0251$ | $n_3 = 124/2 = 62$ | $n_3/n_0 = 0.0239$ |
| $n_4 = 1050/(2\times5) = 105$ | $n_4/n_0 = 0.1055$ | $n_4 = 540/2 = 270$ | $n_4/n_0 = 0.1040$ |
| $n_5 = 690/6 = 115$ | $n_5/n_0 = 0.1156$ | $n_3/n_0 + n_4/n_0 =$ | $n_5/n_0 = 0.1279$ |
| $\longrightarrow$ | $n_1/n_0 = 0.8242$ | $\longrightarrow$ | $n_1/n_0 = 0.8286$ |
| $n_0 = 995^b$ | | $n_0 = 2595^b$ | |

[a] $n_2 = n_{2a} + n_{2b} + n_{2c}$. [b] The ratio 995/2595 is consistent with the change in attenuation (AT) and in vertical scale (VS) of the plots (Figure 6): $995/2595 = (0.75 \times 1062)/(1 \times 2075)$.

Considering the experimental errors, these results demonstrate that the composition of a solution thermolyzed at 92 °C for a period of 24 h is in good agreement with the composition that one predicts using the kinetic parameters deduced from the analysis of the thermograms, assuming three consecutive reactions (CALIT-3). One has, however, to note that the mole fraction of compound **3** is much too high with respect to the calculated value (by a factor of 3!). Indeed the experimental value $n_3/n_0$ does not fit with the relation $n_3/n_0 = n_5/n_0 - n_4/n_0$. Using this relation, it is possible to evaluate a value of $n_3/n_0$ that is compatible with the one predicted by the assumed kinetics: by subtracting $\langle n_4/n_0 \rangle$ from $n_5/n_0$ one obtains $n_3/n_0 = 0.0109 \pm 0.0008$, which is a value that is close to the predicted figure. Note also that the progress of the reaction, measured as $1 - (n_1/n_0) = 0.1736$, is in excellent agreement with the predicted value of 0.1730 in spite of the fact that the error for the experimental value of $n_1/n_0$ is cumulative.

## VII. Short Description of the Simulation Programs CALIT-2 and CALIT-3

The calorimeter used in this study is linearly programmed in temperature and is of the differential type. Its description, its calibration, all its research capabilities, and the exploitation of the thermograms are presented in a book in preparation.[4] We will briefly indicate here the principles of the evaluation of the thermograms.

The calorimeter construction is designed to allow a very accurate mesurement of the heat transfer between the heating block and the reference and sample cells. It is thus possible to deduce the heat flux due to a chemical reaction $\dot{Q}_r$ as a function of time and, by a convenient correction, as a function of the sample temperature $T$. Comparison of the experimental heat flux due to the reaction(s) $\dot{Q}_r(T)$ with theoretical values calculated by integration of the kinetic equations requires a fixed model for the kinetics.

Program CALIT-2[2,4] considers a single isomerization reaction. Three parameters have to be determined: the total reaction heat $Q_{r,tot}$ and the kinetic parameters $E_a$ and $A$. The total heat is obtained initially by total integration of the thermogram. The rate constant $k(T)$ can be estimated from partial integrations of the thermogram. Initial values of $E_a$ and $A$ are obtained from a linear regression of log $k(T)$ versus $1000/T$. The parameters $Q_{r,tot}$, $E_a$ and $A$ are then refined by simulating the thermogram through numerical integration of the kinetic equation and determining parameter changes that optimize the simulation. The optimization is stopped when the quadratic error $\sum_{\text{all points}}(\dot{Q}_{exp} - \dot{Q}_{calc})^2$ ceases to decrease.

Program CALIT-3[3,4] is a generalization of CALIT-2 to the case of successive isomerization reactions. It is also possible to include parallel isomerization reactions. A model for the kinetics must be assumed. For each reaction three parameters must be found: the reaction heat $Q_{r,i}$ and the corresponding Arrhenius parameters $E_{a,i}$ and $A_i$ ($i$ = reaction index). Initial values of these parameters are estimated in a semiquantitative way from the shape of the thermogram: the number and importance of maxima and minima, areas between minima, and so on. These values are used for launching an iterative simulation procedure based on numerical integration of the kinetic equations. The optimization of the parameters ends when the total quadratic error ceases to decrease. Owing to the complexity of the problem, the optimization strategy is based upon the SPIRAL algorithm proposed by Jones.[38] This algorithm has been implemented in CALIT-3 by Dr. J. Heinzer. At the end of the iterative computation, the program CALIT-3 calculates and gives in the output the following:

(1) the refined values of $Q_{r,tot}$, $Q_{r,i}$, $E_{a,i}$, log $A_i$, and, for preselected temperatures, the values of $k_i$, $\Delta H^{\ddagger}_i$, $\Delta S^{\ddagger}_i$, and $\Delta G^{\ddagger}_i$;

(2) a listing of the experimental $\dot{Q}_{exp}$ and the calculated data $\dot{Q}_{calc}$ and a graphic in which the thermograms $\dot{Q}_{exp}(T)$ and $\dot{Q}_{calc}(T)$ are plotted on a common temperature scale (sample temperature $T$);

(3) a graphic in which the errors $\dot{Q}_{exp} - \dot{Q}_{calc}$ (on an enlarged scale) are plotted against $T$;

(4) a graphic representing the evolution of the mole fractions of the different compounds implicated in the reaction mechanism as a function of the sample temperature $T$.

The graphical representation of the errors allows one to conclude whether the proposed mechanism governing the kinetics is the correct one or not; the error distribution has to be statistical.

## VIII. The Kinetic Equations and Their Integration

Let us consider the reactions in Scheme 3. We will assume that the "compound" **2** plays kinetically the role of a single compound, although it consists of three enantiomeric pairs of formulae **2a, 2b**, and **2c**.

Let us designate by $n_1$, $n_2$, $n_3$, $n_4$, and $n_5$ the numbers of moles of compounds **1** ... **5** and by $n_0$ the number of moles of **1** involved in the thermolysis. The kinetic equations expressing the time evolution of the number of moles of each compound are

$$dn_1/dt = -k_1 n_1$$

$$dn_2/dt = k_1 n_1 - k_2 n_2$$

$$dn_3/dt = k_2 n_2 - k_3 n_3$$

$$dn_5/dt = k_2 n_2$$

$$dn_4/dt = k_3 n_3$$

The integration of these equations between the limits $t = 0$ and $t$ gives, after transformations

$$n_1 = n_0 \exp(-k_1 t)$$

$$n_2 = n_0 \frac{k_1}{k_2 - k_1}[\exp(-k_1 t) - \exp(-k_2 t)]$$

$$n_3 = n_0 \frac{k_1 k_2}{k_2 - k_1}\left[\frac{\exp(-k_1 t) - \exp(-k_3 t)}{k_3 - k_1} - \frac{\exp(-k_2 t) - \exp(-k_3 t)}{k_3 - k_2}\right]$$

$$n_5 = n_0 \frac{k_1 k_2}{k_2 - k_1}\left[\frac{1 - \exp(-k_1 t)}{k_1} - \frac{1 - \exp(-k_2 t)}{k_2}\right]$$

$$n_4 = n_0 \left\{\frac{k_2 k_3}{(k_2 - k_1)(k_3 - k_1)}[1 - \exp(-k_1 t)] - \frac{k_1 k_3}{(k_2 - k_1)(k_3 - k_2)}[1 - \exp(-k_2 t)] + \frac{k_1 k_2}{(k_3 - k_1)(k_3 - k_2)}[1 - \exp(-k_3 t)]\right\}$$

A verification of these equations is made by ckecking that they fulfill the following conditions:

$$n_1 + n_2 + n_3 + n_4 = n_0 \quad \text{and} \qquad n_3 + n_4 = n_5$$

**Acknowledgment.** We acknowledge, with gratitude, the financial support of the *Sweizerischer Nationalfonds zur Förderung der Wissenschaftlichen Forschung* and the computing center of the *Eidg. Techn. Hochschule Zürich* for the computing time.

## References and Notes

(1) Oth, J. F. M.; Bünzli, J.-C.; de Julien de Zélicourt, Y. *Helv. Chim. Acta* **1974**, *57*, 2276.

(2) Gilles, J.-M. *Program CALIT-2 (Fortran)*, 1967.

(3) Gilles, J.-M. *Program CALIT-3 (Fortran)*, 1970 and extended by J. Heinzer in 1980 with the "spiral algorithm" as developped by A. Jones (cf. ref 38).

(4) Technical details concerning our calorimeter and the thermogram evaluation methods will appear in a book in preparation: Oth, Jean F. M.; Gilles, Jean-Marie. *Un calorimètre à température programmée permettant la mesure rapide de la fonction capacité calorifique $dH_X/dT$ dans le domaine des températures comprises entre 100 K et 700 K ainsi que la mesure du flux thermique dû à la chaleur de réactions chimiques et des paramètres cinétiques qui les caractérisent.*

(5) Oth, J. F. M.; Röttele, H.; Schröder, G. *Tetrahedron Lett.* **1970**, *1*, 61. Oth, J. F. M.; Gilles, J.-M. *Tetrahedron Lett.* **1970**, *1*, 67. Oth, J. F. M.; Schröder, G. *J. Chem. Soc. B* **1971**, *5*, 904.

(6) Oth, J. F. M. Unpublished results.

(7) Stöckel, K.; Garrat, P. J.; Sondheimer, F.; de Julien de Zélicourt, Y.; Oth, J. F. M. *J. Am. Chem. Soc.* **1972**, *94*, 8644.

(8) de Julien de Zélicourt, Y.; Oth, J. F. M. Results reported in: de Julien de Zélicourt, Y. Ph.D. Thesis, ETH 5679, Zürich, 1976.

(9) Cox, J. D.; Pilcher, G. *Thermochemistry of Organic and Organometallic Compounds;* Academic Press: London and New York, 1970.

(10) Janz, G. J. *Thermodynamic Properties of Organic Compounds;* Academic Press: New York and London, 1967.

(11) Franklin, J. L. *Ind. Eng. Chem.* **1949**, *41*, 1070.

(12) Wiberg, K. B. *Determination of Organic Structures by Physical Methods;* Academic Press: New York and Lodon, 1971; Vol. 3, p 207.

(13) Benson, S. W. *Thermochemical Kinetics;* John Wiley & Sons, Inc.: New York, 1968.

(14) Beezer, A. E.; Mortimer, C. T.; Springall, H. D.; Sondheimer, F.; Wolovsky, R. *J. Chem. Soc.* **1965**, 216.

(15) Mortimer, C. T. *Reaction Heats and Bond Strengths;* Pergamon Press: Oxford−London−New York−Paris, 1962; Chapter 4.

(16) Gilles, J.-M.; Oth, J. F. M.; Sondheimer, F.; Woo, E. P. *J. Chem. Soc. B* **1971**, *11*, 2171.

(17) Oth, J. F. M. *Pure Appl. Chem.* **1971**, *25* (3), 573−622.

(18) de Julien de Zélicourt, Y.; Oth, J. F. M. To be published. The results of the $^{13}$C-NMR study of the conformational mobility in [18]annulene are reported in: de Julien de Zelicourt, Y. Ph.D. Thesis, #5679, ETH, Zürich, 1976.

(19) Mortimer, C. T. *Reaction Heats and Bond Strengths;* Pergamon Press: Oxford−London−New York−Paris, 1962; Chapter 3.

(20) Bregman, J.; Hirshfeld, F. L.; Rabinovich, D.; Schmidt, G. M. J. *Acta Crystallogr.* **1965**, *19*, 227. Hirshfeld, F. L.; Rabinovich, D. *Acta Crystallogr.* **1965**, *19*, 235.

(21) Cottrel, T. L. *The strengths of the chemical bonds,* 2nd ed.; Butterworths: London, 1958. Wilson; Decius; Cross. *Molecular Vibrations;* McGraw Hill: 1955; p 175.

(22) Woodward, R. B.; Hoffman, R. *The Conservation of Orbital Symmetry;* Verlag Chemie: Weinheim, 1971. Anh, N. T. *Les règles de Woodward-Hoffmann;* Ediscience: Paris, 1970.

(23) The terms "isodynamic" and "isometric" were introduced by: Altman, S. L. *Proc. R. Soc. London, Ser. A* **1967**, *298*, 184.

(24) Enantiomers with same nuclei labeling are counted as two isometric structures.

(25) Longuet-Higgins, H. C. *Mol. Phys.* **1963**, *6*, 445.

(26) Herzberg, G. *Molecular Spectra and Molecular Structure;* Van Nostrand: Princeton, NJ, 1945.

(27) Salthouse, J. A.; Ware, M. J. *Point group character tables and related data,* Cambridge University Press: New York, 1972.

(28) We will adopt shorter names to identify compounds **3** and **4**.

(29) Benson, S. W.; O'Neal, E. H. *Kinetic Data on Gas Phase Unimolecular Reactions;* NSRDS-NBS 21; National Bureau of Standards: (Gaithersburg, MD) 1970; pp 268−272 and references cited therein.

(30) Neuman, M.; Roth, W. Data quoted and discussed in: Neuman M. Ruhr Universität Bochum, 1994.

(31) Oth, J. F. M. *Union Carbide ERA Tech. Memorandum,* No. 27; Union Carbide European Research Associates: Brussels, 1970.

(32) Baumann, H.; Cometta-Morini, C.; Oth, J. F. M. *J. Mol. Struct.: THEOCHEM* **1986**, *138*, 229−237.

(33) Bischof, P. K. *J. Am. Chem. Soc.* **1976**, *98*, 6844.

(34) Pople, J. A.; Nesbet, R. K. *J. Chem. Phys.* **1954**, *22*, 571.

(35) Salotto, A. W.; Burnelle, L. *J. Chem. Phys.* **1970**, *52*, 2936.

(36) Philipps, D. H.; Schug, J. C. *J. Chem. Phys.* **1974**, *61*, 1031.

(37) Dewar, M. J. S. *J. Am. Chem. Soc.* **1984**, *106*, 209.

(38) Jones, A. *Comput. J.* **1970**, *13*, 301.